ORIGINAL PAPER

Studies of interaction of tumor suppressor p53 with apo-MT using surface plasmon resonance

Ning Xia · Lin Liu · Xinyao Yi · Jianxiu Wang

Abstract The interaction of tumor suppressor p53 with apo-metallothionein (apo-MT) has been carried out using a flow injection-surface plasmon resonance (FI-SPR) instrument. MT was first tethered onto the carboxymethylated dextran film. Via incorporation of glycine–HCl (pH 2) to remove the sequestrated metal ions inherent in MT molecules, a more extended and open structure of apo-MT was formed. Substantial SPR angle shift corresponding to the interaction of wild-type p53 with apo-MT was observed. The interaction was originated from the binding between the free sulfhydryl groups of apo-MT and Zn^{2+} of p53 with the binding constant of $1.4 \times 10^8 M^{-1}$. The specific binding of p53 to consensus double-stranded DNA was hindered after metal chelation from p53 by apo-MT. Furthermore, inhibition of the interaction between p53 and apo-MT imposed by p53/DNA complex was observed. The fluorescence measurements also revealed the binding of p53 to apo-MT, being consistent with the SPR results. Thus, SPR could potentially serve as an attractive technique for monitoring p53 conformational change and transcriptional activity regulated by the MT/apo-MT couple.

Keywords Surface plasmon resonance · Metallothionein · p53 · Interaction

N. Xia · L. Liu · X. Yi · J. Wang (✉)
School of Chemistry and Chemical Engineering,
Central South University,
Changsha, Hunan 410083, People's Republic of China
e-mail: jxiuwang@mail.csu.edu.cn

Introduction

The tumor suppressor p53 is the most frequently mutated gene, playing important roles in maintenance of genome integrity [1, 2]. The inactivation of p53 could lead to the development of more than half of human cancers [3, 4]. The human p53 protein comprises three major functional domains: N-terminal domain (residues 1–94), a central DNA-binding domain (102–292), and C-terminal oligomerization domain (311–364) [2]. The mutation hotspots in various human cancers are confined in the DNA-binding domain and almost all of the biological functions of p53 are related to its DNA-binding property [5, 6]. p53 usually forms as a tetramer which binds to the consensus double-stranded (ds-) DNA with a sequence of PuPuPuC(A/T)(T/A)GPyPyPy (where Pu and Py represent purines and pyrimidines, respectively) [7–9]. The DNA-binding domain contains a zinc-finger-like motif in which one zinc ion is tetrahedrally coordinated to three cysteines and one histidine [5]. The zinc ions are requisite for maintenance of wild-type p53 conformation, stability and its sequence-specific DNA-binding activity [10, 11].

Metallothionein (MT) is a low-molecular-weight and cysteine-rich protein capable of regulating essential metals, detoxifying nonessential metals, and scavenging free radicals [12, 13]. Apo-MT, the metal-free form of MT, was formed via treatment with an acidic solution [14] or transiently generated in the cell through biochemical manipulations [10, 15]. It has been reported that the MT/apo-MT couple could modulate metal transfer of several biological species, such as estrogen receptor, TFIIIA, SP1, mitochondrial aconitase, and p53 [10, 16–20]. Furthermore, biological activities of metalloproteins including p53 could be regulated via zinc chelation [10, 19, 21]. In certain tumor cells, the presence of mutant p53 was found to be related to

high expression of MT [22, 23]. Thus, potential relationship should exist between p53 and MT. As reported by Ostrakhovitch EA et al., a complex between apo-MT and wild-type or mutant p53 was formed in breast cancer epithelial cells [17]. Such an interaction was monitored by co-immunoprecipitation using antibodies to probe the immunoprecipitates and western blot analysis for bands visualization [17]. Moreover, the interaction between p53 and apo-MT results in the conformational change of p53 with loss of DNA-binding activity [10]. Immunoprecipitation was utilized to probe the protein conformation and the DNA-binding activity was determined by electro-mobility-shift assay using a ^{32}P-labeled p53^{CS} sequence [10]. However, these methods either involve complicated assay procedures and severe experimental conditions, or the use of antibodies or labeled analytes. Thus, it is highly desirable to develop a simple, label-free, and sensitive technique that can conveniently determine the interaction of p53 with apo-MT and the influence of the incorporated DNA on such an interaction.

Surface plasmon resonance (SPR) is an optical technique suitable for measuring the thickness and structure of ultrathin adsorbate layers at metal films [24, 25]. Biosensors based on SPR have been demonstrated as an attractive means for rapid, sensitive, and label-free analysis of biomolecular interactions [26–28]. Furthermore, binding kinetic analysis of the biomolecular interactions can be conducted using SPR [29, 30]. Zhou et al. reported the metal ion binding by surface-confined apo-MT using a highly sensitive SPR spectrometer [31]. In another work by the same author, real-time detection of Cu^{2+} sequestration and release by immobilized apo-MT was accomplished using scanning electrochemical microscopy combined with SPR [32]. Campagnolo C et al. reported the qualitative SPR measurement of the interaction between the immobilized histidine-tagged p53 and antibodies in serum [33]. In this work, interaction of p53 with apo-MT was monitored by SPR. The influence of the incorporated DNA on such an interaction was also investigated.

Experimental

Chemicals and materials

Rabbit liver Zn$_7$MT was acquired from Hunan Lugu Biotech Co., Ltd (Changsha, China). Tris(hydroxymethyl) aminomethane hydrochloride (Tris–HCl), N-(3-dimethylaminopropyl)-N′-ethylcarbodiimide hydrochloride (EDC), N-hydroxysuccinimide (NHS), ethylenediaminetetraacetic acid disodium salt (EDTA), cystamine hydrochloride, glycine, 1, 4-dithiothreitol (DTT), ethanolamine hydrochloride (EA), NaCl, KH$_2$PO$_4$, and K$_2$HPO$_4$ were acquired

from Sigma-Aldrich. Carboxymethylated dextran sodium salt was obtained from Fluka. Microcon YM-3 centrifugal filter units with a molecular weight cutoff of 3 kDa were purchased from Millipore Corp. (Belleria, MA). DNA samples were obtained from Shanghai Sangon Co., LTD (Shanghai, China). The sequences of 25-mer oligodeoxynucleotide (ODN) probe with its 5′ end modified with amino groups and its complementary target to form the consensus ds-ODN are 5′-H$_2$N-(CH$_2$)$_6$-TTT TTA GAC ATG CCC AGA CAT GCC C-3′, and 5′-GGG CAT GTC TGG GCA TGT CT-3′, respectively. The ODNs used to form the non-consensus ds-ODN have sequences of 5′-H$_2$N-(CH$_2$)$_6$-TTT TTG TCG GCC GAG GTC GGC CGA G-3′ and 5′-CTC GGC CGA CCT CGG CCG AC-3′, respectively. Recombinant p53 sample was purchased from BD Biosciences Pharmingen (San Diego, CA). Other reagents were all from commercial sources with analytical purity and used as received. All experiments were performed at room temperature (25±1°C).

Instruments

The FI-SPR measurements were conducted with a BI-SPR 1000 system (Biosensing Instrument Inc, Tempe, AZ). Phosphate-buffered saline (PBS buffer, 10 mM phosphate/10 mM NaCl, pH 7.4) was degassed and used as the carrier solution. The samples were preloaded into a 50-μL sample loop on a six-port valve and then delivered to the flow cell with a low volume of 2.5 μL by a Genie Plus syringe pump (Kent Scientific, Torrington, CT) at a flow rate of 10 μL/min.

Procedures

Solution preparation

Apo-MT used in the fluorescence measurements was prepared by acidifying Zn$_7$MT with glycine–HCl (pH 2) and then filtering the mixture with the YM-3 membrane. The released metal ions eluted through the pores of the membrane and became separated from the MT species. To minimize oxidation of free thiols of apo-MT, the metal-free protein was prepared right before each experiment and dissolved in PBS buffer containing 5 mM DTT. Similarly, recombinant p53 was diluted with PBS buffer containing 5 mM DTT. Deionized water was used to prepare the DNA probe solution. DNA target was prepared with TNE buffer (10 mM Tris–HCl, 1.0 mM EDTA, and 0.1 M NaCl, pH 7.0).

SPR sensor surface modification with MT/apo-MT

The SPR sensor fabrication and modification were carried out as follows. The deposition of Au film with 50-nm thickness and 2-nm Cr underlayer onto the pretreated glass

slides (BK7, Fisher) was carried out with a sputter coater (model 108, Kurt J. Lesker, Clairton, PA, USA). Prior to surface modifications, the gold films were annealed in a hydrogen flame to eliminate surface contamination. The procedure for SPR assay via injection of glycine–HCl and then p53 onto the sensor chip pre-covered with MT is illustrated in Fig. 1. Cystamine self-assembled monolayers (SAMs) were formed by immersing the gold film into 10 mM of cystamine hydrochloride solution overnight. Via the widely used EDC/NHS chemistry [34], carboxymethylated dextran molecules were tethered onto the preformed cystamine SAMs upon soaking the film into a mixture comprising 10 mg/ml dextran, 75 mM EDC, and 15 mM NHS for 3 h. The hydrogel-like dextran layer was used to eliminate nonspecific adsorption of p53 molecules and to offer higher binding capacity. As depicted in Fig. 1a, MT was immobilized onto the dextran film by casting a mixture of EDC, NHS, and 50 μM MT onto the chip surface for 2.5 h. The unreacted NHS ester groups were treated with 1 M EA for 15 min. After each step, the surface was rinsed with a copious amount of deionized water to rid any residual molecules and dried with N_2. Apo-MT-covered sensor chip was obtained by injecting glycine–HCl (pH 2) onto the MT-modified substrate to remove the sequestrated metal ions inherent in MT molecules, thus resulting in a linear structure of apo-MT [31] (Fig. 1b). The acid treatment has no effect on the hydrogel-like dextran layer and the thiol/Au bond, being consistent with those reported previously [31, 35].

SPR sensor surface modification with consensus ds-ODN

Immobilization of the ODN capture probe modified with amino groups was carried out by casting a mixture of 2 μM ODN probe, 75 mM EDC, and 15 mM NHS onto the preformed dextran film. Via treatment of the unreacted NHS terminal groups with EA, ds-DNA formation was accomplished by dropping 2 μM of ODN target onto the ODN probe-modified substrate and the hybridization reaction was allowed to proceed for 3 h.

SPR detection

Upon completion of the surface modifications, the film was assembled onto the SPR prism with an index-matching fluid (Type A immersion oil, Cargille Laboratories, Cedar Grove, NJ, USA). Once a stable baseline had been obtained, recombinant p53 sample was delivered to the SPR flow cell by the syringe pump. The signals that report on the binding of p53 with MT, apo-MT, and consensus ds-DNA were measured by BI-SPR 1000 system. The conversion of SPR angle shift to degree was carried out using the ethanol calibration method [36]. Based on the work on the quantitative interpretation of the responses of SPR sensors to adsorbed films by Campbell et al. [37], refractive index unit (RIU) was used to describe the SPR angle shift. The interconversion of the SPR angle shift in degrees with RIU follows the following relationship: 1×10^{-6} RIU$=7.3 \times 10^{-5}$ degree based on the BI-SPR 1000 system.

Fluorescence measurement

The fluorescence of p53 in the absence and presence of MT or apo-MT was determined using a Hitachi F-2500 spectrofluorometer (Tokyo, Japan). The excitation wavelength was set at 280 nm. All spectra were background-corrected.
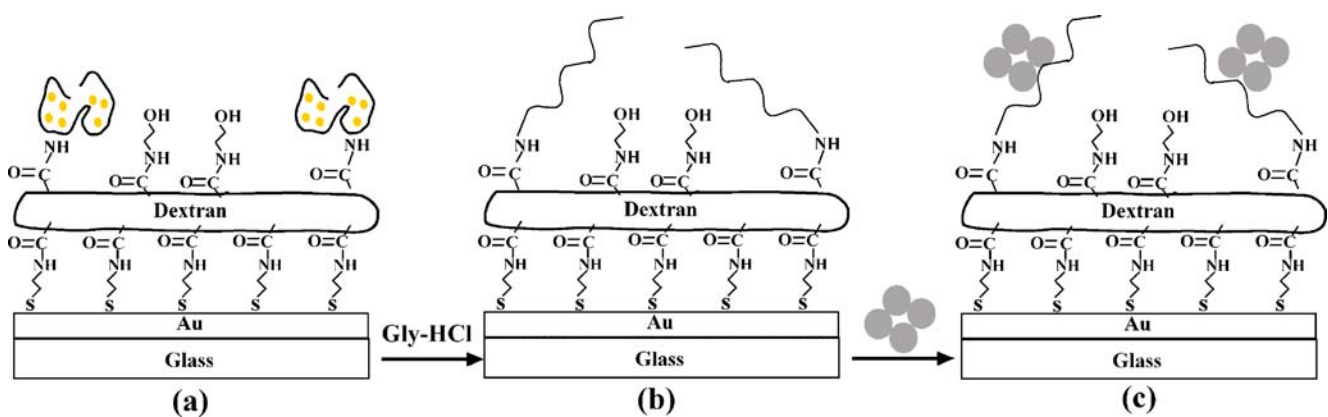

Fig. 1 Schematic representation of MT immobilization (**a**), metal release from MT-covered sensor chip (**b**), and interaction of apo-MT-modified SPR substrate with recombinant p53 (**c**). The dumbbell-like structure in (**a**) represents the MT molecules. The exposure of MTs to an acidic solution caused the MT adsorbates to possess a more extended and open structure (**b**). The tetramer in *gray color* in (**c**) represents the p53 molecules. For clarity, all molecules are not drawn to scale

Results and discussion

Interaction of apo-MT/MT with p53

Figure 2 is an overlay of three typical SPR sensorgrams upon injecting 50 μL of 0.56 nM recombinant p53 solution into the flow cell housing apo-MT (curve a), MT (curve b), and carboxymethylated dextran (curve c) -covered sensor chips. After recombinant p53 had been replaced by the carrier solution, a new baseline was established in curve a with SPR angle being higher than the original value. The SPR angle shift, deduced from the difference in the baseline of SPR angles, is about 0.0088° in curve a (1.21×10^{-4} RIU). However, due to the elimination of nonspecific adsorption of p53 molecules by the hydrogel-like dextran layer, the SPR angle remains essentially unchanged at the substrates covered with MT (curve b) and carboxymethylated dextran (curve c). In all the three cases, the transient increase in SPR angle is caused by the refractive index change between the sample and the carrier solution. DTT did not yield significant SPR angle shift (data not shown), but prevented oxidation of the metal-free cysteine thiols at the surface of the p53 molecules [38, 39]. It has been reported that treatment of MTs with an acidic solution would result in extraction of the pristine metal ions inherent in MTs [14]. Thus, via exposure of MT-covered sensor chip to glycine–HCl (pH 2), the adsorbed MTs would adopt a more extended and open structure in response to the unfolding of the dumbbell-like structure (Fig. 1b). The incorporation of glycine was anticipated to chelate metal ions released from MT molecules and to replace the metal-coordination sites with protons [40]. With the introduction
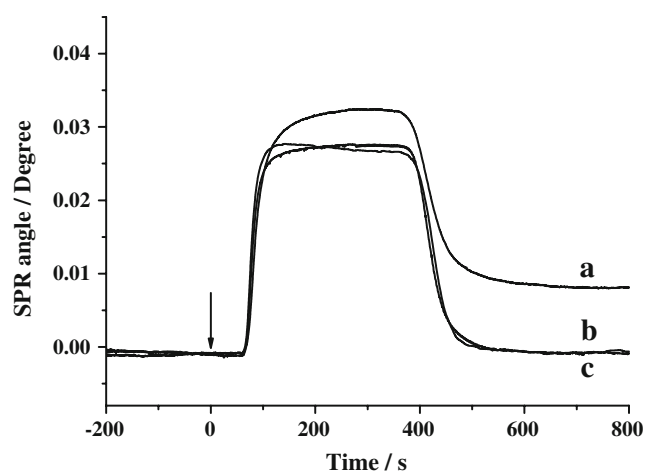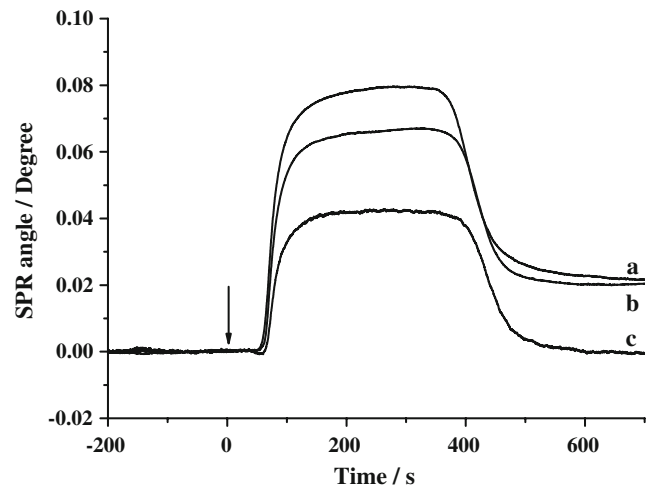
Fig. 3 Time-resolved SPR sensorgrams acquired by injecting a mixture of 1.0 nM recombinant p53 and 500 nM MT (a), 1.0 nM recombinant p53 (b), and a mixture of 1.0 nM p53 and 500 nM apo-MT (c) onto the substrates pre-covered with consensus ds-DNA. A flow rate of 10 μL/min was used. The *arrow* indicates the time when the injection was made
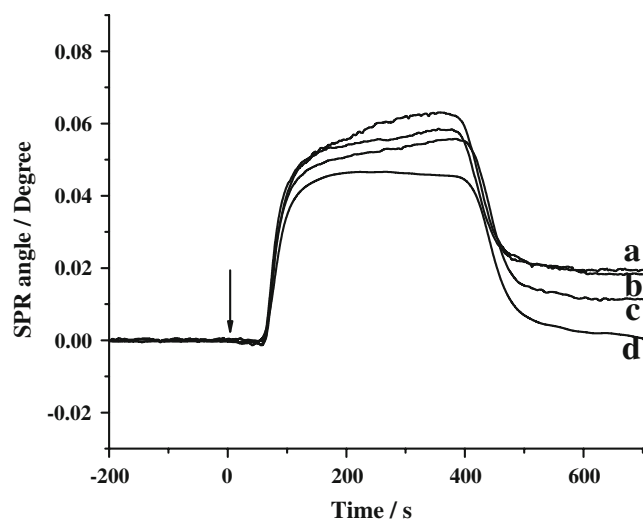
of recombinant p53 onto the substrate pre-covered with apo-MT, a complex could be formed due to the interaction between the free sulfhydryl groups of apo-MT and Zn^{2+} of p53 (Fig. 1c). But in the case of MT, no such interaction should be observed. This is in accordance with a previous report [17]. The DNA-binding domain of p53 comprises a zinc-finger motif in which a zinc atom is tetrahedrally coordinated to three cysteines and one histidine [5, 10]. Metal chelation from p53 by apo-MT would result in the conformational change of p53 from the wild-type to the "mutant like" form and hence the loss of sequence-specific DNA-binding activity [10, 17]. Such an interaction could be easily and sensitively monitored by SPR. The extraction of zinc ion of p53 by apo-MT concords with that reported for TFIIIA, Spl, and estrogen receptor zinc finger by apo-MT [16, 18, 20, 21].

The relatively high binding affinity has an interesting implication with respect to the interaction between apo-MT and p53. The binding process of apo-MT to p53 could be monitored in real-time by SPR, thus providing direct insight into the interaction. The affinity constant was determined by simulating a series of binding curves recorded at different p53 concentrations. The equilibrium association constant was estimated to be $1.4 \times 10^{8} M^{-1}$ based on a 1:1 type of biomolecular interaction, suggesting that apo-MT binds strongly to p53.

Binding of p53 to consensus ds-DNA or apo-MT hindered by the preformed complex

The zinc ions are essential for maintenance of wild-type p53 conformation, stability, and its sequence-specific DNA-

Fig. 2 Time-resolved SPR sensorgrams acquired by injecting 50 μL of 0.56 nM recombinant p53 solution onto the various substrates covered with apo-MT (a), MT (b), and carboxymethylated dextran (c), respectively. The *arrow* indicates the time when the injection was made

Fig. 4 Time-resolved SPR sensorgrams acquired by injecting 2.8 nM recombinant p53 (**a**), a mixture of 2.8 nM p53 and 25 nM non-consensus ds-DNA (**b**), a mixture of 2.8 nM p53 and 25 nM ss-DNA (**c**), a mixture of 2.8 nM p53 and 25 nM consensus ds-DNA (**d**) onto the substrates pre-covered with apo-MT. A flow rate of 10 μL/min was used. The *arrow* indicates the time when the injection was made

binding activity [10]. To assess the binding affinity of p53 to consensus ds-DNA after metal chelation from p53 by apo-MT, wild-type p53 was pre-incubated with excess amounts of apo-MT or Zn_7MT for 30 min. Figure 3 is an overlay of three SPR sensorgrams acquired upon injecting 50 μL of recombinant p53 solution in the absence or presence of MT or apo-MT onto the substrates covered with consensus ds-DNA. The SPR angle shifted by 0.0220° in curve b (3.02×10^{-4} RIU), which resulted from the specific binding of wild-type p53 to the consensus ds-DNA [41]. The exposure of consensus ds-DNA-covered sensor chip to the mixture of p53 and MT caused an SPR angle shift of 0.0239° (3.28×10^{-4} RIU) (curve a). The small variation in SPR angle shift in curves a and b suggests that MT had a

negligible influence on the binding of p53 to ds-DNA. However, little change in the baseline of curve c was observed after the mixture of p53 and apo-MT had been replenished out of the fluidic channel, indicating that specific binding of p53 to the consensus ds-DNA was hindered by apo-MT. The hindrance was attributed to the sequestration of zinc ion of p53 by apo-MT, which induced p53 to adopt a disrupted and unfolded form with loss of DNA-binding activity [10]. We also performed an experiment in which 500 nM MT was injected onto the same consensus ds-ODN-covered sensor chip used in curve a of Fig. 3, no significant SPR angle shift was observed (data not show), indicating that MT does not nonspecifically adsorb onto the consensus ds-ODN-covered surface.

The results suggest that interaction of apo-MT with wild-type p53 prevented further binding of p53 to the consensus ds-DNA. In order to examine whether the preformed p53/DNA complex had a similar effect on the interaction of p53 with apo-MT, wild-type p53 was pre-incubated with excess amounts of consensus ds-DNA for 30 min, and the mixture was injected onto the apo-MT-covered sensor chip. As shown in curve d in Fig. 4, once the mixture of p53 and consensus ds-DNA completely eluted out of the flow cell, the SPR baseline returned to the original level. This suggests that via binding to consensus ds-DNA, p53 loses its ability to further interact with apo-MT, being consistent with the case of TFIIIA and apo-MT [18]. It is known that the zinc-finger motif is located in the DNA-binding domain of p53, thus the steric hindrance imposed by p53/ds-DNA complex might have impeded the further reaction of p53 with apo-MT. Note that the SPR angle shift induced by recombinant p53 (curve a) was larger than that by the mixture of p53 and single-stranded (ss)-DNA (curve c). Such a difference was attributable to the nonspecific binding of ss-DNA to p53 [42, 43]. We also conducted an experiment in which the apo-MT-modified sensor chip was
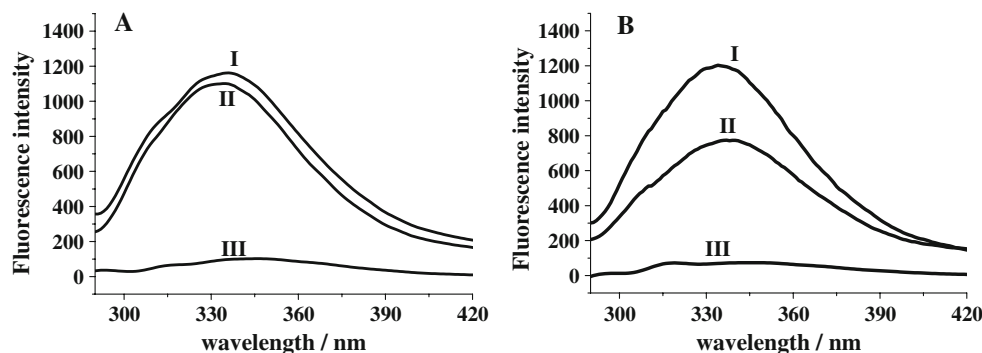
Fig. 5 Fluorescence emission spectra of 40 nM wild-type p53 in the absence of both MT and apo-MT (*curve I*, **A** and **B**), and in the presence of 10 μM MT (*curve II*, **A**) or 10 μM apo-MT (*curve II*, **B**) in 10 mM PBS buffer comprising 5 mM DTT. The background signals for MT (*curve III*, **A**) and apo-MT (*curve III*, **B**) were also shown. The excitation wavelength was set at 280 nm. Prior to each measurement, p53 solution was incubated with apo-MT or MT for 20 min

exposed to a mixture of p53 and non-consensus ds-DNA (curve b), essentially the same SPR angle shift as that in curve a suggests that non-consensus ds-DNA has a negligible influence on the interaction between p53 and apo-MT.

Fluorescence measurement of the interaction of MT/apo-MT with p53

Alternatively, the interaction of tumor suppressor p53 with apo-MT can be monitored by fluorescence spectroscopy. Fluorescence of the tryptophan residues in the N-terminal domain of p53 has been used to monitor conformational change imposed by protein unfolding [44]. As shown in Fig. 5, wild-type p53 displayed a typical emission peak at 336 nm, characteristic of the tryptophan residues [45, 46] (curve I, A and B). The addition of apo-MT leads to a significant decrease in the fluorescence signal (curve II, B), indicating the conformational change of wild-type p53 induced by the interaction. However, relatively small fluorescence variation was obtained in the case of MT (curve II, A). The fluorescence measurements were in good agreement with the SPR results.

Conclusions

Interaction of tumor suppressor p53 with apo-MT was investigated using SPR. Upon injection of recombinant p53 onto the apo-MT covered sensor chip, substantial SPR angle shift was observed. However, no interaction was obtained in the case of MT. The interaction was ascribed to the strong binding between free sulfhydryl groups of apo-MT and Zn^{2+} of p53 with the binding constant estimated to be $1.4\times10^8 M^{-1}$. The binding of p53 to consensus ds-DNA after metal chelation from p53 by apo-MT was also examined and the specific binding of p53 to the consensus ds-DNA was hindered by apo-MT. The hindrance was attributed to the unfolding of wild-type p53 with the accompanying loss of DNA-binding activity. On the other hand, the preformed p53/DNA complex had a similar effect on the interaction between p53 and apo-MT. The fluorescence measurements also showed the conformational change of wild-type p53 upon addition of apo-MT, being in line with the SPR results. The above results indicate that SPR could be utilized as a potential technique to monitor the conformational change and transcriptional activity of p53 modulated by the MT/apo-MT couple.

References

1. Levine AJ (1997) Cell 88:323–331
2. May P, May E (1999) Oncogene 18:7621–7636
3. Kastan MB, Onyekwere O, Sidransky D, Vogelstein B, Craig RW (1991) Cancer Res 51:6304–6311
4. Fritsche M, Haessler C, Brandner G (1993) Oncogene 8:307–318
5. Cho YJ, Gorina S, Jeffrey PD, Pavletich NP (1994) Science 265:346–355
6. Prives C (1994) Cell 78:543–546
7. Clore GM, Omichinski JG, Sakaguchi K, Zambrano N, Sakamoto H, Appella E, Gronenborn AM (1994) Science 265:386–391
8. Eldeiry WS, Kern SE, Pietenpol JA, Kinzler KW, Vogelstein B (1992) Nat Genet 1:45–49
9. Sturzbecher HW, Brain R, Addison C, Rudge K, Remm M, Grimaldi M, Keenan E, Jenkins JR (1992) Oncogene 7:1513–1523
10. Méplan C, Richard MJ, Hainaut P (2000) Oncogene 19:5227–5236
11. Verhaegh GW, Parat MO, Richard MJ, Hainaut P (1998) Mol Carcinog 21:205–214
12. Hamer DH (1986) Annu Rev Biochem 55:913–951
13. Margoshes M, Vallee BL (1957) J Am Chem Soc 79:4813–4814
14. Hunziker PE (1991) Methods Enzymol 205:451–452
15. Jacob C, Maret W, Vallee BL (1998) Proc Natl Acad Sci USA 95:3489–3494
16. Zeng J, Heuchel R, Schaffner W, Kagi JHR (1991) FEBS Lett 279:310–312
17. Ostrakhovitch EA, Olsson PE, Jiang S, Cherian MG (2006) FEBS Lett 580:1235–1238
18. Huang M, Shaw CF, Petering DH (2004) J Inorg Biochem 98:639–648
19. Feng W, Cai J, Pierce WM, Franklin RB, Maret W, Benz FW, Kang YJ (2005) Biochem Biophys Res Commun 332:853–858
20. Cano-Gauci DF, Sarkar B (1996) FEBS Lett 386:1–4
21. Zeng J, Vallee BL, Kagi JHR (1991) Proc Natl Acad Sci USA 88:9984–9988
22. Cherian MG, Jayasurya A, Bay B-H (2003) Mutat Res 533:201–209
23. Rainwater R, Parks D, Anderson ME, Tegtmeyer P, Mann K (1995) Mol Cell Biol 15:3892–3903
24. Tao N, Boussaad S, Huang W, Arechabaleta RA, D'Agnese J (1999) Rev Sci Instrum 70:4656–4660
25. Economou EN (1969) Phys Rev 182:539–554
26. Song F, Zhou F, Wang J, Tao N, Lin J, Vellanoweth RL, Morquecho Y, Wheeler-Laidman J (2002) Nucleic Acids Res 30:e72
27. Endo T, Kerman K, Nagatani N, Hiepa HM, Kim DK, Yonezawa Y, Nakano K, Tamiya E (2006) Anal Chem 78:6465–6475
28. Shumaker-Parry JS, Aebersold R, Campbell CT (2004) Anal Chem 76:2071–2082
29. Faegerstam LG, Frostell-Karlsson A, Karlsson R, Persson B, Roennberg I (1992) J Chromatogr 597:397–410
30. Myszka DG (1997) Curr Opin Biotechnol 8:50–57
31. Zhang Y, Xu M, Wang Y, Toledo F, Zhou F (2007) Sens Actuators B: Chem 123:784–792
32. Xin Y, Gao Y, Guo J, Chen Q, Xiang J, Zhou F (2008) Biosen Bioelectron 24:369–375
33. Campagnolo C, Meyers KJ, Ryan T, Atkinson RC, Chen Y-T, Scanlan MJ, Ritter G, Old LJ, Batt CA (2004) J Biochem Biophys Methods 61:283–298
34. Huang E, Zhou F, Deng L (2000) Langmuir 16:3272–3280
35. Roden LD, Myszka DG (1996) Biochem Biophys Res Commun 225:1073–1077

36. Kolomenskii AA, Gershon PD, Schuessler HA (1997) Appl Opt 36:6539–6547
37. Jung LS, Campbell CT, Chinowsky TM, Mar MN, Yee SS (1998) Langmuir 14:5636–5648
38. Makmura L, Hamann M, Areopagita A, Furuta S, Munoz A, Momand J (2001) Antioxid Redox Signal 3:1105–1118
39. Sun X, Vinci C, Makmura L, Han S, Tran D, Nguyen J, Hamann M, Grazziani S, Sheppard S, Gutova M, Zhou F, Thomas J, Momand J (2003) Antioxid Redox Signal 5:655–665
40. Bontidean I, Berggren C, Johansson G, Csoregi E, Mattiasson B, Lloyd JA, Jakeman KJ, Brown NL (1998) Anal Chem 70:4162–4169
41. McLure KG, Lee PWK (1999) EMBO J 18:763–770
42. Wang J, Zhu X, Tu Q, Guo Q, Zarui CS, Momand J, Sun X, Zhou F (2008) Anal Chem 80:769–774
43. Bakalkin G, Yakovleva T, Selivanova G, Magnusson KP, Szekely L, Kiseleva E, Klein G, Terenius L, Wiman KG (1994) Proc Natl Acad Sci USA 91:413–417
44. Bullock AN, Henckel J, DeDecker BS, Johnson CM, Nikolova PV, Proctor MR, Lane DP, Fersht AR (1997) Proc Natl Acad Sci USA 94:14338–14342
45. Nichols NM, Matthews KS (2001) Biochem Biophys Res Commun 288:111–115
46. Bell S, Hansen S, Buchner J (2002) Biophys Chem 96:243–257